Optimum Threshold Parameter Estimation of Wavelet Coefficients Using Fisher Discriminant Analysis for Speckle Noise Reduction

Mohammad Motiur Rahman[1], Mithun Kumar PK[1] and Mohammad Shorif Uddin[2]
[1]Department of Computer Science and Engineering, MBSTU, Bangladesh
[2]Department of Computer Science and Engineering, Jahangirnagar University, Bangladesh

Abstract: *Optimizing threshold value of wavelet coefficient is an important task in speckle noise reduction in the wavelet domain. Without proper selection of threshold value image information may be lost, which is unwanted. In this paper we proposed optimum threshold parameter using Fisher Discriminant Analysis (FDA) for determining the optimum threshold value of wavelet coefficient for the best speckle noise reduction. It also preserves edges without destroying image information. The method is compared with the several other classical thresholding methods on variety of images and the experimental results confirm significant improvement over existing methods.*

Keywords: *FDA, optimum threshold, speckle noise, ultrasound image, wavelet.*

Received July 20, 2012; accepted June 4, 2013; published online March 13, 2014

1. Introduction

Image denoising is one of the most significant and fundamental tasks for image preprocessing. The aim of the image denoising algorithm is to reduce the noise level as well as preserving the important image features or information. Speckle is a particular kind of multiplicative noise which occurs in images obtained by coherent imaging systems like ultrasound. It tends to degrade the resolution and contrast of ultrasound images, thus may lead to eliminate some useful and important diagnostic information. In the recent years there has been a fair amount of research on wavelet thresholding for signal denoising because wavelet provides appropriate basis for separating noise signal from image signal. The main challenge of this method is to find an optimum threshold value because a small threshold value will pass all the noisy coefficients and hence the resultant denoised signal may still be noisy. On the other hand, a large threshold value makes more number of coefficients as zero which leads to smooth signal and destroys details and image may produce blur and artifacts. Many wavelet based thresholding techniques like hard thresholding, soft thresholding, VisuShrink, SureShrink, BayesShrink and Bayes thresholding [1, 3, 4, 5, 6, 7, 8, 9, 10, 11, 13, 16] have proved better efficiency in image processing. Bayes thresholding is selected by maximum likelihood estimation.

Fisher Discriminant Analysis (FDA) [2] has been widely applied in pattern recognition and classification. For that it is sometime necessary for finding threshold value. In papers [2, 15] FDA is used for selecting optimum threshold value for pattern recognition and classification. In [17] wavelet based denoising preprocessing with FDA scheme is proposed for fault diagnosis. In this paper we proposed FDA based thresholding method for denoising speckle noise of different images. Figure 1 shows a simple flow diagram of our system.

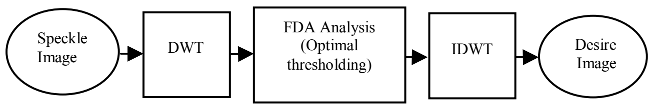

Figure 1. Block diagram of the proposed FDA technique for accurate speckle noise reduction and the best edge preservation approach for ultrasound image.

The paper is organized as follows: In section 2, we define the ultrasound speckle suppression problem by outlining the speckle noise model and the FDA. Section 3 describes wavelet transformation and wavelet shrinkage. Section 4 the numerical implementation scheme of the proposed FDA optimal threshold method is presented. Section 5 presents the evaluation criteria for checking the filter performance. Section 6 compares the performance of the proposed method with other existing speckle noise reduction methods.

2. Theoretical Background

2.1. Speckle Noise Model

Denote by a noisy observation $I(x, y)$ (i.e., the recorded ultrasound image) of the Two-Dimensional (2D) function $f(x,y)$ (i.e., the noise-free image that has to be recovered) and by $\eta_{m(x,y)}$ and $\eta_{a(x,y)}$ the corrupting multiplicative and additive speckle noise components, respectively. One can write:

$$I(x, y) = f(x, y) \times \eta_m (x, y) + \eta_a (x, y) \tag{1}$$

Generally, the effect of the additive component of the speckle in ultrasound images is less significant than the effect of the multiplicative component. Thus, ignoring the term $\eta_a(x, y)$, one can rewrite Equation 1 as:

$$I(x, y) = f(x, y) \times \eta_m (x, y) \tag{2}$$

To transform the multiplicative noise model into an additive one, we apply the logarithmic function on both sides of Equation 2.

2.2. Fisher Discriminant Analysis

FDA locates directions efficient for discrimination by yielding the maximum ratio of between-class scatter to within-class scatter. For each image Fisher Linear Discriminant (FLD) finds a projection orientation of intensity by which two classes (object and background) are well separated. For any image, there is a set X including N intensity.

$$\begin{gathered} X = \{ C1, C2 \} = \{ x_1, x_2, \ldots, x_n \} \\ n1 + n2 = N \end{gathered} \tag{3}$$

Where $n1$ and $n2$ are cardinality of subset $C1$ and subset $C2$ respectively. If we form a linear combination of the components of x_i. We obtain:

$$y_i = w^T x_i \tag{4}$$

Of all the possible lines we would like to select the one that maximizes the separability of the scalars. In order to find a good projection vector, we need to define a measure of separation. The mean vector of each class in x space and y space is:

$$\mu_i = \frac{1}{N_i} \Sigma x \in \omega_i \, x \tag{5}$$

And

$$\tilde{\mu}_i = \frac{1}{N_i} \Sigma y \in \omega_i \, y = \frac{1}{N_i} \Sigma x \in \omega_i \, W^T x = W^T \mu_i \tag{6}$$

We can then choose the distance between the projected means as our objective function:

$$J(W) = \left| \tilde{\mu}_1 - \tilde{\mu}_2 \right| = \left| W^T (\mu_1 - \mu_2) \right| \tag{7}$$

However, the distance between projected means is not a good measure since, it does not account for the standard deviation within classes. Fisher suggested maximizing the difference between the means, normalized by a measure of the within-class scatter. For each class we define the scatter, an equivalent of the variance, as:

$$\tilde{s}_i^2 = \Sigma y \in \omega_i (y - \tilde{\mu}_i)^2 \tag{8}$$

Where the quantity $(\tilde{S}_1^{\,2} + \tilde{S}_2^{\,2})$ is called the within-class scatter of the projected examples. The FLD is defined as the linear function $W^T x$ that maximizes the criterion function:

$$J(W) = \frac{\left| \tilde{\mu}_1 - \tilde{\mu}_2 \right|^2}{\tilde{S}_1^{\,2} + \tilde{S}_2^{\,2}} \tag{9}$$

Therefore, we are looking for a projection examples from the same class are projected very close to each other and, at the same time, the projected means are as farther apart as possible. To find the optimum W, first we define a measure of the scatter in feature space x:

$$s_i = \Sigma x \in \omega_i (x - \mu_i)(x - \mu_i)^T \tag{10}$$

$$S_1 + S_2 = S_W \tag{11}$$

Where S_W is called the within class scatter matrix. The scatter of the projection y can then be expressed as a function of the scatter matrix in feature space x:

$$\begin{aligned} \tilde{s}_i^2 &= \Sigma y \in \omega_i (y - \tilde{\mu}_i)^2 = \Sigma x \in \omega_i (W^T x - W^T \mu_i)^2 \\ &= \Sigma x \in \omega_i W^T (x - \mu_i)(x - \mu_i)^T W = W^T S_i W \end{aligned} \tag{12}$$

$$\tilde{S}_1^{\,2} + \tilde{S}_2^{\,2} = W^T S_w W \tag{13}$$

Similarly, the difference between the projected means can be expressed in terms of the means in the original feature space:

$$\begin{aligned} (\tilde{\mu}_1 - \tilde{\mu}_2)^2 &= (W^T \mu_1 - W^T \mu_2)^2 \\ &= W^T (\mu_1 - \mu_2)(\mu_1 - \mu_2)^T W = W^T S_B W \end{aligned} \tag{14}$$

The matrix S_B is called the between class scatter. Note that, since S_B is the outer product of two vectors, its rank is at most one. We can finally express the fisher criterion in terms of S_W and S_B as:

$$J(W) = \frac{W^T S_B W}{W^T S_W W} \tag{15}$$

To find the maximum of $J(W)$ we derive and equate to zero:

$$\begin{gathered} \frac{d}{dw}[J(W)] = \frac{d}{dw}\left[\frac{W^T S_B W}{W^T S_W W}\right] = 0 \Rightarrow \\ \left[W^T S_W W\right] \frac{d\left[W^T S_B W\right]}{dw} - \left[W^T S_B W\right] \frac{d\left[W^T S_W W\right]}{dw} = 0 \Rightarrow \\ \left[W^T S_W W\right] 2 S_B W - \left[W^T S_B W\right] 2 S_W W = 0 \end{gathered} \tag{16}$$

Dividing by $W^T S_W W$:

$$\begin{gathered} \left[\frac{W^T S_W W}{W^T S_W W}\right] S_B W - \left[\frac{W^T S_B W}{W^T S_W W}\right] S_W W = 0 \Rightarrow \\ S_B W - J S_W W = 0 \Rightarrow \\ S_W^{-1} S_B W - J W = 0 \end{gathered} \tag{17}$$

Solving the generalized eigen value problem yields $S_W^{-1} S_B W = JW$:

$$W^* = \operatorname{argmax} \left[\frac{W^T S_B W}{W^T S_W W}\right] S_W^{-1} (\mu_1 - \mu_2) \tag{18}$$

This is knows as FLD.

3. Wavelet Technique

3.1. Wavelet Transform

2D scaling and wavelet functions are used for wavelet transformation. The scaled and translated basis functions are:

$$f_{j,m,n}(x,y) = 2^{j/2} f(2^j x - m, 2^j y - n) \quad (19)$$

$$\psi^i_{ju,m,n}(x,y) = 2^{j/2} \psi^i(2^j x - m, 2^j y - n) \quad (20)$$

Where: $i=\{H,V,D\}$.

The Discrete Wavelet Transform (DWT) of function *f(x, y)* of size $M\times N$ then:

$$W_f(j_0,m,n) = \frac{1}{\sqrt{MN}} \sum_{x=0}^{M-1}\sum_{y=0}^{N-1} f(x,y) f_{j_0,m,n}(x,y) \quad (21)$$

$$W^i_\psi(j,m,n) = \frac{1}{\sqrt{MN}} \sum_{x=0}^{M-1}\sum_{y=0}^{N-1} f(x,y) \psi^i_{j,m,n}(x,y) \quad (22)$$

Where: $i=\{H,V,D\}$.

We get four subband coefficient values from image for applying DWT. Those subbands are Approximation and Detail, Detail includes horizontal, vertical, diagonal. If we want to get the previous data then have to perform the inverse operation. The Inverse Discrete Wavelet Transform (IDWT) is:

$$f(x,y) = \frac{1}{\sqrt{MN}} \sum_m \sum_n W_f(j_0,m,n) f_{j_0,m,n}(x,y) + \frac{1}{\sqrt{MN}} \sum_{i=H,V,D} \sum_{j=j_0}^{\infty} \sum_m \sum_n W^i_\psi(j,m,n) \psi^i_{j,m,n}(x,y) \quad (23)$$

After execution of IDWT data will come back previous state and construct the original data.

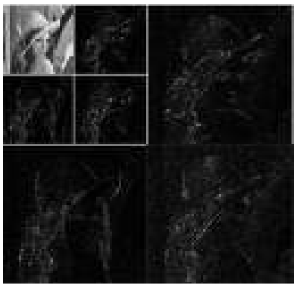

Figure 2. Two-level decomposition of Lena image.

3.2. Wavelet Shrinkage

Let *W(.)* and $W^{-1}(.)$ denote the forward and inverse wavelet transform operators. Let $D(., \lambda)$ denote the thresholding operator with threshold λ. The practice of thresholding denoising consists of the following three steps:

- *Step 1*: $Y=W(x)$
- *Step 2*: $Z=D(Y,\lambda)$
- *Step 3*: $\hat{x} = W^{-1}(Z)$

Hard thresholding and soft thresholding are only different in step 2.

3.2.1. Hard Thresholding

In the case of hard thresholding:

$$D(Y,\lambda) = \begin{cases} Y & \text{if } \|Y\| > \lambda \\ 0 & \text{otherwise} \end{cases} \quad (24)$$

3.2.2. Soft Thresholding

In the case of soft thresholding, or Wavelet shrinkage:

$$D(Y,\lambda) = \begin{cases} \text{sign}(Y)(\|Y\| - \lambda) & \text{if } \|Y\| > \lambda \\ 0 & \text{otherwise} \end{cases} \quad (25)$$

3.2.3. Bayes Shrink

The observation model is $Y = X + V$, with X and V independent of each other, hence:

$$\sigma_Y^2 = \sigma_X^2 + \sigma^2 \quad (26)$$

Where the noise variance σ^2 is estimated from the subband *HH*1 by the robust median estimator [14]:

$$\sigma = \frac{Median(|Y_{ij}|)}{0.6745}, \; Y_{ij} \in subband \quad HH_1 \quad (27)$$

And σ_Y^2 is the variance of *Y*. Since, *Y* is modeled as zero-mean, σ_Y^2 can be found empirically by:

$$\hat{\sigma}_Y^2 = \frac{1}{n} \sum_{i,j=1}^{n} Y_{ij}^2 \quad (28)$$

Where $n\times n$ is the size of the subband under consideration. Thus:

$$\hat{T}_B(\hat{\sigma}_X) = \frac{\hat{\sigma}^2}{\hat{\sigma}_X} \quad (29)$$

Where: $\hat{\sigma}_X = \sqrt{max(\hat{\sigma}_Y^2 - \hat{\sigma}^2, 0)}$

4. Proposed Method

4.1. Objective Function

Firstly discrete wavelet transform is applied on an image for creating the subband coefficient. An image is *f(x, y)* and the size of image is $M\times N$ then DWT is:

$$W^i_\psi(j,m,n) = \frac{1}{\sqrt{MN}} \sum_{x=0}^{M-1}\sum_{y=0}^{N-1} f(x,y) \psi^i_{j,m,n}(x,y) \quad (30)$$

Where: $i=\{H,V,D\}$

<table>
<tr><td>A3</td><td>H3</td><td rowspan="2">H2</td><td rowspan="3">H1</td></tr>
<tr><td>V3</td><td>D3</td></tr>
<tr><td colspan="2">V2</td><td>D2</td></tr>
<tr><td colspan="3">V1</td><td>D1</td></tr>
</table>

Figure 3. Subbands of the 2D orthogonal wavelet transform.

Where (H1, V1, D1); (H2, V2, D2) and (H3, V3, D3) are 1, 2 and 3 scale wavelet coefficient subband respectively. Individually each coefficient is denoted by n_i. Total number of coefficient $N = n_0 + n_1 + n_2 + \ldots$

$+ n_M$. Now, we have to calculate each coefficient probability using below this equation:

$$P_i = \frac{n_i}{N}; \quad P_i \, 0 \tag{31}$$

Where: $\sum_{i=0}^{M} P_i = 1$

Suppose that the coefficients are divided into two classes C1 and C2 by a fixed value t; C1 is the set of coefficients with levels *[0, 1, ..., L]*, and the rest of coefficients belong to C2. C1 and C2 normally correspond to the object class and the back ground one, or vice versa. Then, the probabilities of the two classes are given by within:

$$W_1(L) = \sum_{i=0}^{L} P_i \qquad W_2(L) = 1 - W_1(L) \tag{32}$$

The mean coefficients of the two classes can be defined as:

$$\mu_1 = \sum_{i=0}^{L} \frac{iP_i}{W_1} \qquad \mu_2 = \sum_{i=L+1}^{M} \frac{iP_i}{W_2} \tag{33}$$

Corresponding class variances are given by:

$$\sigma_1^2 = \sum_{i=0}^{L} \frac{(i-\mu_1)^2 P_i}{W_1} \qquad \sigma_2^2 = \sum_{i=L+1}^{M} \frac{(i-\mu_2)^2 P_i}{W_2} \tag{34}$$

The within-class variance can be defined [12]:

$$\sigma_W^2 = W_1\sigma_1^2 + W_2\sigma_2^2 \tag{35}$$

As we have seen in section 2.2, the FLD seeks directions efficient for discrimination by yielding the maximum ratio of between-class scatter to within-class scatter. Thus, Based on the function defined by Equation 9 the following criterion as objective function to evaluate the separability of the threshold at level L.

$$\rho(L) = \frac{(\mu_1(L) - \mu_2(L))^2}{\sigma_W^2} \tag{36}$$

Where: $\sigma_W^2 = W_1\sigma_1^2 + W_2\sigma_2^2$

From Equation 33 we shall get FDA thresholding value T between two classes as follows. T can be used for separating two classes but, if we want to apply threshold value T for noise reduction then this type of thresholding can not be efficient for noise reduction. These situations we can overcome by applying the standard deviation and mean value ratio of the coefficient of any subband of the wavelet. Here we proposed the proper threshold value estimation method for speckle noise reduction in the wavelet domain. So, this method is given below.

If the discrete wavelet transform of function is $\xi(x, y)$ and the image size is $F \times H$ then the mean value of the wavelet coefficient is:

$$\mu_c = \frac{1}{F \times H} \sum \xi^i(x, y) \tag{37}$$

Where: $i = \{H, V, D\}$

And the standard deviation of the wavelet coefficient is:

$$\sigma_c = \sqrt{\frac{\sum_{x=0}^{F-1}\sum_{y=0}^{H-1}[\xi(x,y) - \mu_c]^2}{F \times H}} \tag{38}$$

For the large FDA threshold value T huge amount of diagnostic information is lost. To remove this limitation we use mathematical operations between mean and standard deviation of wavelet coefficients with respect to FDA threshold value to obtain an optimal threshold value. The proposed optimal threshold value is:

$$T_{optimal} = \frac{T}{\sqrt{\left|\frac{\sigma_c}{\mu_c}\right|}} \tag{39}$$

Where: $\left|\frac{\sigma_c}{\mu_c}\right| > 0$

Now, we get optimal threshold value from Equation 36 using FDA for speckle noise reduction of ultrasound images. We know $\xi^i(x, y)$ is the discrete wavelet coefficient and optimal threshold value is $T_{optimal}$. Optimal threshold operation on wavelet coefficient is shown below:

$$\begin{aligned} &\text{If } \xi^i(x, y) < T_{optimal} \quad i = \{H, V, D\} \\ &\quad \text{then } \xi^i(x, y) = 0 \\ &\text{End} \end{aligned}$$

Table 1. For Liver ultrasound image.

Method	SNR	EPF	MSE
FDA thresholding (T)	13.3880	0.1745	7.2077
FDA optimal thresholding ($T_{optimal}$)	17.7252	0.6972	2.2166

We use "Lena" image for testing the performance between FDA thresholding and FDA optimal thresholding. From Table 1 we see that FDA optimal thresholding exhibits better performance than FDA thresholding. Here we show the histogram comparison and efficiency of those threshold values.

From Figure 4, we see that Figure 4-b lost its structural view but, Figure 4-c has a structural view with respect to original image. We observe that FDA optimal threshold show the better performance for edge preservation over existing FDA threshold. Very small amount of error occurred in the filtered image for FDA optimal thresholding technique and enhance the image clearly. From these measurements, we can comment that FDA optimal threshold performance significantly better than FDA threshold.

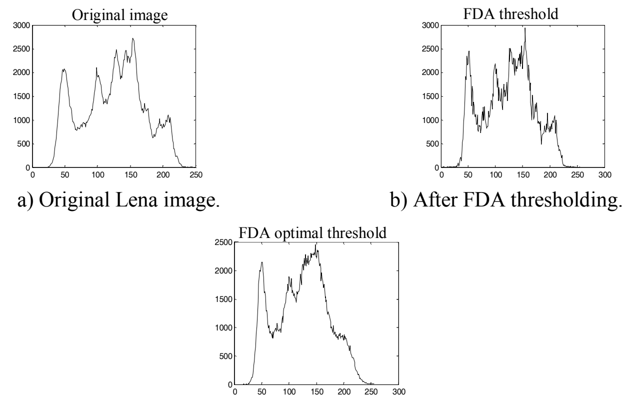

a) Original Lena image. b) After FDA thresholding.

c) After FDA optimal thresholding.

Figure 4. Histogram of Lena image with FDA thresholding operation.

4.2. Algorithm

Following steps describe the proposed algorithm for image denoising:

1. Let $max_p=0$, be the maximum value of the objective function.
2. For $k=0$ to Maximum of coefficient value.
3. Compute the objective function value corresponding to the coefficient value k:

$$\begin{aligned} &If\ \ max_{\rho} < \rho(k)\\ &\quad then\ \ max_{\rho} = \rho(k)\\ &\qquad T = k\\ &End \end{aligned}$$

4. The optimal threshold value estimation for denoising in wavelet field:

$$T_{optimal} = \frac{T}{\sqrt{\left|\frac{\sigma_c}{\mu_c}\right|}}$$

Where: $\left|\frac{\sigma_c}{\mu_c}\right| > 0$

5. Wavelet coefficient is denoted by W_c and Optimal threshold value performance is:

If Wc< Toptimal
then Wc=0
End

5. Evaluation Criteria

We observe the performance by apply Signal to Noise Ratio (SNR), Mean Square Error (MSE) and Edge Preservation Factor (EPF) parameter [14]. Signal to Noise Ratio (SNR):

$$SNR = -10log10\left[\frac{\sum_{x=1}^{M}\sum_{y=1}^{N}(I_d(x,y) - I(x,y))^2}{\sum_{x=1}^{M}\sum_{y=1}^{N}(I_d(x,y))^2}\right] \quad (40)$$

The edge preservation ability of the filter is compared by EPF and is computed using EPF:

$$EPF = \frac{\sum(\Delta I - \overline{\Delta I})(\Delta I_d - \overline{\Delta I_d})}{\sqrt{\sum(\Delta I - \overline{\Delta I})^2(\Delta I_d - \overline{\Delta I_d})^2}} \quad (41)$$

Where ΔI and ΔI_d are the high pass filtered versions of images I and I_d, obtained with a 3×3 pixel standard approximation of the Laplacian operator. The larger value of EPF means more ability to preserve edges. MSE:

$$MSE = \left[\frac{1}{M \times N}\sum_{x=0}^{M-1}\sum_{y=0}^{N-1}(I(x,y) - I_d(x,y))^2\right] \quad (42)$$

Where the image size is $M \times N$. x means row, y means column, I means original image and I_d means filtered image.

6. Experimental Result

The proposed algorithm has been applied to 2D ultrasound image with have been corrupted by multiplicative noise (speckle noise of variance 0.004). The computation is carried out on MATLAB 7.12.0.635(R2011a) in a Core 2 duo 2.33GHz and 1GB RAM desktop having a Windows operating system. We choose four images (e.g., Cameraman, Lena, Kidney, Liver) for testing the performance of the proposed algorithm. Our proposed algorithm is compared with existing method which is shown in Tables 2 and 3 and Figures 8, 9 and 10 respectively.

Table 2. For cameraman and lena images.

Method	Cameraman			Lena		
	SNR	EPF	MSE	SNR	EPF	MSE
Wavelet Hard Threshold	24.0790	0.3781	6.8536	22.3069	0.2273	5.8765
Wavelet Soft Threshold	24.3232	0.4052	6.4791	22.8611	0.2892	5.1722
Bayesian Threshold	25.3662	0.5122	5.0974	23.8748	0.4370	4.0986
FDA Denoising	27.9296	0.7129	2.9955	26.5587	0.6949	2.9883

Table 3. For ultrasound kidney and liver images

Method	Kidney			Liver		
	SNR	EPF	MSE	SNR	EPF	MSE
Wavelet Hard Threshold	8.5828	0.2554	4.7968	14.6471	0.3443	4.9520
Wavelet Soft Threshold	8.5253	0.2532	4.8029	14.6147	0.3636	4.9625
Bayesian Threshold	8.5949	0.3471	4.5668	14.6950	0.4622	4.8874
FDA Denoising	11.1302	0.5934	2.7511	17.7252	0.6972	2.2166

Experimental numerical results show the improved speckle noise reduction capabilities of the proposed FDA optimal threshold based filtering compared to the classical methods. From Tables 2 and 3, we see that our proposed filter effectively and properly remove speckle noise from ultrasound images because a small amount of error is occurred in the filter image and the proposed method is shown the mentionable edge preservation.

Histogram of the wavelet coefficient is given below:

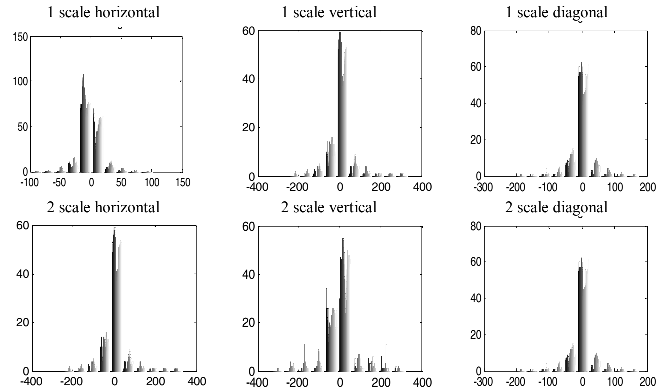

a) Histogram of Cameraman image.

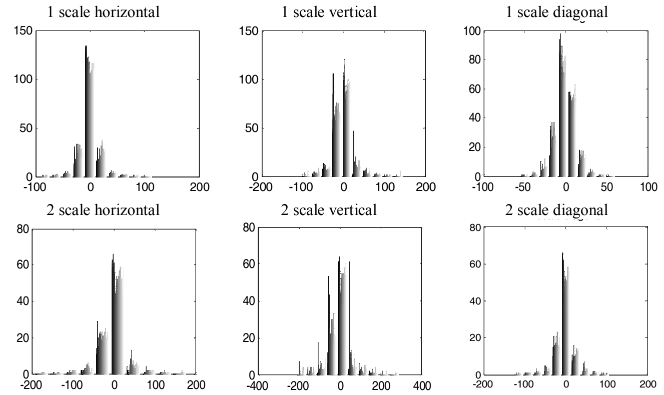

b) Histogram of Lena image.

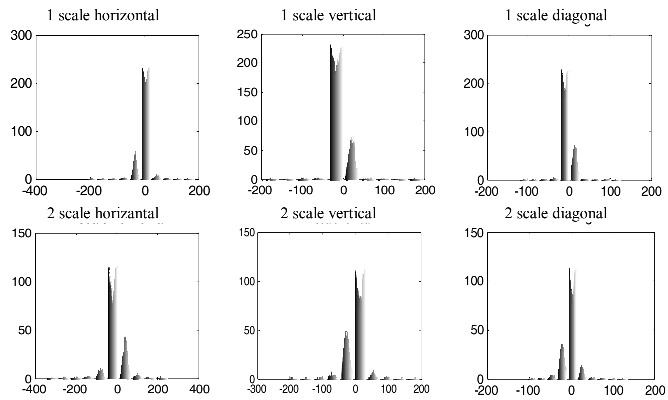

c) Histogram of Kidney image.

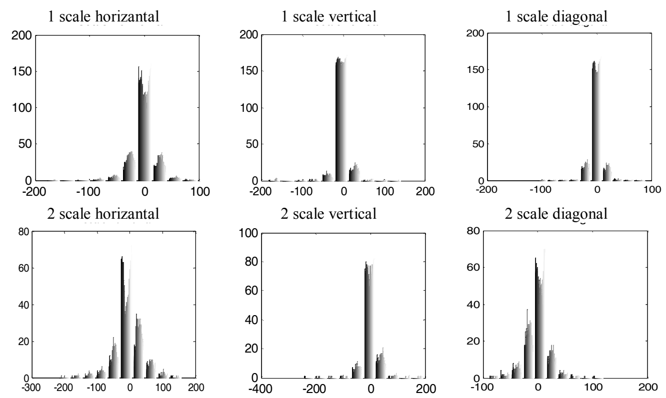

d) Histogram of Liver image.

Figure 5. Histogram of the wavelet coefficients of four test images.

Figure 5 mainly depicts the coefficient variation of the wavelet domains by the histograms. We observe from these histograms that the coefficient variation of the diagonal subband is always smaller than other Detail. Diagonal subbands are more sensitive for optimal threshold value estimation and noise analysis or reduction.

Probability density curve of original image and filter image is given below:

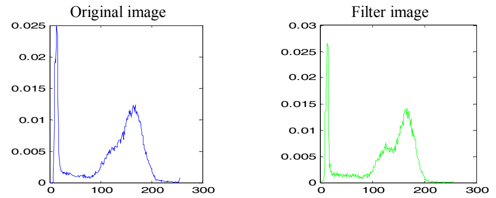

a) Probability density curves of Cameraman image.

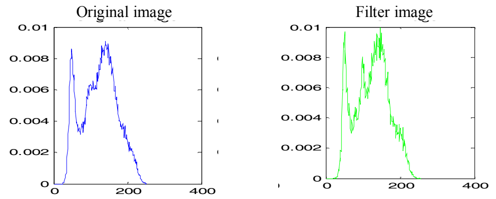

b) Probability density curves of Lena image.

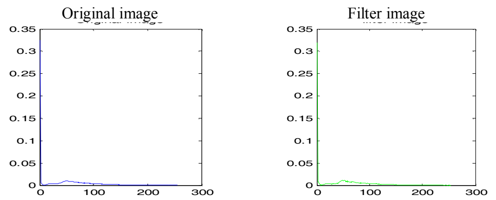

c) Probability density curves of Kidney image.

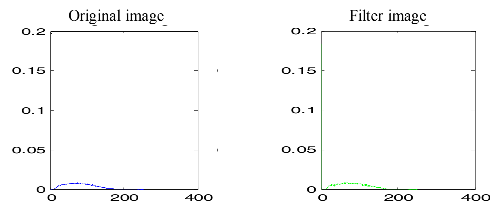

d) Probability density curves of Liver image.

Figure 6. Probability density curves of four test images.

We can see that from the probability density curves Figure 6 of original and filter images, very small change between two curves. So, we can say that a small amount of information is lost and very small amount of error is occurred in the filter image. Naturally filter image is so structural that means the edge preservation and smoothness of the filter image is really good with respect to original image.

Mean and variance curves of two classes (e.g. between class scatter, within class scatter) only for diagonal (D) subbands are given below.

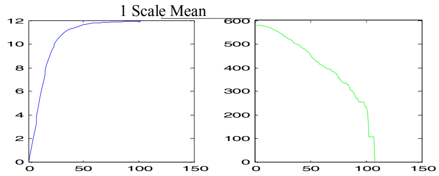

a) Mean curves of Cameraman image for the first level diagonal.

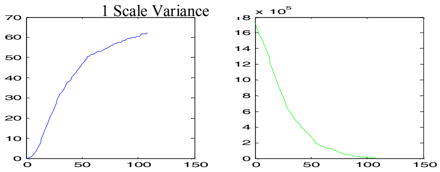

b) Variance curves of Cameraman image for the first level diagonal.

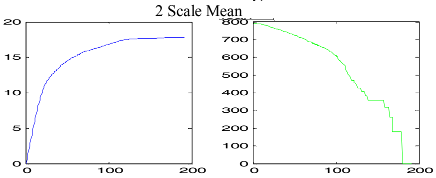

c) Mean curves of Cameraman image for the second level diagonal.

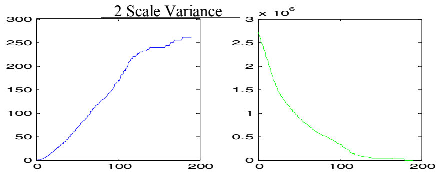

d) Variance curves of Cameraman image for the second level diagonal.

Figure 7. Mean and variance curve of diagonal coefficient of Cameraman image.

Figure 7 is used for measuring the central tendency to the natural or original structure of the filtered data of between class scatter and within class scatter using mean value and variance.

Visual quality comparison is given below for 2 levels:

a) Lena noisy image.

b) Hard Thresholding.

c) Soft Thres2holding.

d) BayesShrink.

e) Bayesian Thresholding.

f) FDA Denoising.

Figure 8. Visual comparison of Lena image after execution some existing state-of-the-art filters and our proposed filter on Lena noisy image.

a) Kidney ultrasound noisy image.

b) Hard Thresholding.

c) Soft Thresholding.

d) BayesShrink.

e) Bayesian Thresholding.

f) FDA Denoising.

Figure 9. Visual comparison of Kidney ultrasound image after execution some existing state-of-the-art filters and our proposed filter on Kidney ultrasound noisy image.

a) Liver ultrasound noisy image.

b) Hard Thresholding.

c) Soft Thresholding.

d) BayesShrink.

e) Bayesian Thresholding.

f) FDA Denoising.

Figure 10. Visual comparison of Liver ultrasound image after execution some existing state-of-the-art filters and our proposed filter on Liver ultrasound noisy image.

From Figures 8, 9, and 10, proposed filtered image visual quality is absolutely good because our proposed algorithm shows better performance for speckle noise reduction. From the observation of the proposed filtered image, we see that it is so smooth and enhance over existing despeckle methods images and its has no any checker board and blurring effect in the homogeneous regions but preserve edges significantly without destroying vital information of the image.

7. Conclusions

We have proposed an effective method for speckle denoising via wavelet transformation using FDA proposed optimal threshold value. Our method exhibits better performance in comparison to existing methods for speckle noise reduction, edge preservation, visual quality and mean squared error. Our proposed method is especially effective for highly inhomogeneous image and can be used widely for speckle noise reduction of speckle affected images.

References

[1] Achim A., Bezeriano A., and Tasakalides P., "Novel Bayesian Multiscale for Speckle Removal in Medical Ultrasound Images," *IEEE Transactions on Medical Imaging Journal*, vol. 20, no. 8, pp.772-783, 2001.

[2] Azim G. and Abo-Eleneen Z., "Thresholding based on Fisher Linear Discriminant," *Journal of Pattern Recognition Research*, vol. 6, no. 2, pp. 326-334, 2011.

[3] Donoho D. and Johnstone I., "Adapting to Unknown Smoothness via Wavelet Shrinkage," *Journal of American the Denoising Performance. Statistical Assoc*., vol. 90, no. 432, pp. 1200-1224, 1995.

[4] Donoho D. and Johnstone I., "Ideal Spatial Adaptation via Wavelet Shrinkage," *Biometrica*, vol. 81, no. 3, pp. 425-455, 1994.

[5] Donoho D. and Johnstone I., "Wavelet Shrinkage: Asymptopia," *Journal of the Royal Statistical Society. Series B*, vol. 57, no. 2, pp. 301-369, 1995.

[6] Fodor I. and Kamath C., "Denoising Through Wavelet Shrinkage," *Journal of Electronic Imaging*, vol. 12, no. 1, pp. 151-160, 2003.

[7] Grace C., Yu B., and Vattereli M., "Adaptive Wavelet Thresholding for Image Denoising and Compression," *IEEE Transaction Image Processing*, vol. 9, no. 9, pp. 1532-1546, 2000.

[8] Grace C., Yu B. and Vattereli M., "Spatially Adaptive Wavelet Thresholding with Context Modeling for Image Denoising," *IEEE Transaction Image Processing*, vol. 9, pp. 1522-1530, 2000.

[9] Grace C., Yu B., and Vattereli M., "Wavelet Thresholding for Multiple Noisy Image Copies," *Journal of IEEE Transaction Image Processing*, vol. 9, pp. 1631-1635, 2000.

[10] Jansen M., "Noise Reduction by Wavelet Thresholding," *Springer-Verlag*, New York, USA, 2001.

[11] Muhsen Z., Dababneh M., and Nsour A., "Wavelet and Optimal Requantization Methodology for Lossy Fingerprint Compression," *the International Arab Journal of Information Technology*, vol. 8, no. 4, pp. 383-387, 2011.

[12] Otsu N., "A Threshold Selection Method from Gray-Level Histograms," *IEEE Transaction System Man Cybern*, vol. 9, no.1, pp 62-66, 1979.

[13] Rajan J. and Kaimal M., "Image Denoising Using Wavelet Embedded Anisotropic Diffusion (WEAD)," *in Proceedings of IEEE International Conference on Visual Engineering(VIE)*, London, UK, pp. 589-593, 2006.

[14] Sattar F., Floreby L., Salomonsson G., and Lovstorm B., "Image Enhancement Based on a Nonlinear Multiscale Method," *IEEE Transactions on Image Processing*, vol. 6, no. 6, pp. 888-895, 1997.

[15] Shaho B., Wang Y., Deng X., and Wang S., "Sparse linear Discriminant Analysis by Thresholding High Dimensional Data," *The Annals of statistics*, vol. 39, no. 2, pp. 1241-1265, 2011.

[16] Vattereli M. and Kovacevic J., *Wavelets and Subband Coding. Englewood Cliffs*, Prentice Hall, New Jersy, USA, 1995.

[17] Wu H. and Huang D., "Kernel Fisher Discriminant Analysis Using Feature Vector Selection for Fault Diagnosis," *in proceedings of the 2nd IEEE international symposium on intelligent information technology application*, Shanghai, China, pp.109-113, 2008.

Mohammad Motiur Rahman received his BSc Engineering and MSc degree in computer science and engineering from Jahangirnagar University, Bangladesh, in 1995 and 2001, where he is currently pursuing the PhD degree. His research interests include digital image processing, medical image processing, computer vision and digital electronics. He has many international journal and conference publications.

Mithun Kumar PK he received his BSc engineering degree in computer science and engineering from Mawlana Bhashani Science and Technology University, Bangladesh. His research interests include image analysis, image processing and medical image processing, pattern recognition, 3D visualization, segmentation, filter optimization. He has many international journal and conference publications and He is a regular reviewer of IET image processing journal.

Mohammad Shorif Uddin is currently working in the Department of Computer Science and Engineering, Jahangirnagar University, Bangladesh. His research is focused on bioimaging and image analysis, computer vision, pattern recognition, blind navigation, medical diagnosis, and disaster prevention. He published many papers in renowned journals like IEEE, Elsevier, IET, Optical Society of America etc.